Simplifying mechanistic impedances

David A. Harrington

April 2020

Citation for this paper:

Harrington, D.A. (2020). Simplifying mechanistic impedances. *Electrochimica Acta, 338*, 135895. https://doi.org/10.1016/j.electacta.2020.135895

Accepted version of Electrochim. Acta, 338 (2020) 135895 doi: 10.1016/j.electacta.2020.135895

Simplifying mechanistic impedances

David A. Harrington*

Department of Chemistry, University of Victoria, Victoria, British Columbia, V8W 3V6, Canada.

Abstract

Common simplifying concepts of chemical kinetics, such as rate-determining and preequilibium steps, can be used to simplify the formulation of the electrochemical impedance for reaction mechanisms. A general strategy for eliminating kinetic parameters of preequilibrium steps from the governing equations is presented, which enables simpler subsequent generation of the impedance spectra and associated equivalent circuits. Examples that are various subcases of a metal electrode with simultaneous hydrogen evolution and hydrogen adsorption into the metal are discussed. The relationship of the apparent charge-transfer resistance to the true charge-transfer resistance is discussed. Examples are given where the presence of adsorption is masked and may not be easily detected in an impedance analysis.

Key words: rate-determining step, equivalent circuits, impedance, Devanathan-Stachurski, absorption, preequilibrium

Introduction

The methodology to derive the electrochemical impedance corresponding to a reaction mechanism involves linearizing the kinetic equations. It has been used for a long time for quite complicated mechanisms, and has been systematized in a matrix form [1–4] so that it is now straightforward to compute the impedance spectrum for any set of reactions and kinetic parameters. There has also been some progress on the inverse problem; deducing which types of mechanisms can correspond to which shapes of impedance spectra, e.g, Ref. 5.

The complexity of the spectrum, in terms of the number of semicircles (loops) in a Nyquist plot or bends in a Bode plot is known to be related to the number of reaction steps with linearly independent stoichiometry [1–4]. According to these rules, a complicated reaction mechanism is expected to give a complicated impedance spectrum at least at some potentials. However, impedance spectra are often deceptively simple, and mask the complexity of the underlying mechanism. This may be because some reaction steps or species do not affect the shape of the spectrum or have no significant role to play, e.g., fast steps after the rate-determining step (RDS). The first systematic approach to simplifying EIS spectra was by Sengoku et al [6], who classified species into those in fast or slow reactions, and noted that the "measurable kinetic parameters are only those of slow reactions modified by fast reactions". They found conditions under which the species in fast reactions could be eliminated from the Jacobian matrix, without specifying the nature of the reactions.

Here I approach the problem in the framework commonly used in general chemical kinetics, where two simplifying methods are common. The first is the steady-state approximation, also called the Bodenstein approximation or adiabatic elimination. This sets the time derivatives of the concentrations of fast intermediates to zero, which allows these concentrations to be eliminated from the kinetics. Since these species are eliminated before linearizing the equations to find the impedance, they are invisible in EIS and do not require special treatment. The second method uses the concepts of the rate-determining step (RDS) and preequilibrium steps, and is the topic of this work. In electrochemistry, this method is widely used to understand Tafel slopes of steady-state polarization curves [7, 8], but has not been much used in EIS. For fitting EIS spectra at a given potential, it is important to reduce the number of parameters to those that can be reliably fitted, or the fitting routine will have difficulty finding a global minimum. The approach is to find general methods to decide how the spectra simplify. This builds on earlier work that showed that if a reaction mechanism with multiple adsorbed species has a single RDS, the impedance collapses to a single semicircle [9].

Understanding how impedances simplify is part of the wider problem of finding diagnostic criteria for reaction mechanisms. Aside from understanding the possible shapes of spectra, it is important also to develop criteria for the potential dependence of measurable parameters to decide which mechanisms might be operating. One strategy is to investigate particular mechanisms and determine ranges of rate constants or other rate parameters that produce particular shapes, for example a single semicircle, e.g., Diard, Montella and coworkers produced zone diagrams for a number of mechanisms [10–15]. These studies give in-

---

*Corresponding author.
Email address: `dharr@uvic.ca` (David A. Harrington)

sights into simple cases where the full behaviour can be characterized by a small number of parameters. A more general strategy is to fit data to equivalent circuits, and then use the potential dependence of the circuit elements to determine which mechanism might apply. This was the approach of Kichigin and Shein [16], who produced diagnostic criteria for potential dependence of the circuit elements for the hydrogen evolution reaction (HER) under simplifying assumptions about which steps are rate determining. They also used the concept of preequilibrium for the Volmer reaction in some of these cases. Lasia also gave examples of simplified mechanisms and equivalent circuits in his recent review of the HER [17].

The concept of the RDS and the simplification of spectra discussed here occur at higher overpotentials. The spectra generally show the greatest structure near equilibrium [18]. Of course, maximum kinetic information is obtained by studying the spectra over a range of potentials while systematically changing relevant solution concentrations.

1. Results and Discussion

Rather than approach the theory from an abstract point of view, I take as an example the case of the hydrogen evolution reaction with possible absorption of hydrogen into the metal electrode, and consider various subcases. The details of the impedance of this mechanism have been reviewed by Lasia [19], and many particular cases have been discussed in the literature, e.g., [20–23]. Here the emphasis is on general strategies for simplifying the mechanism.

$$\mathrm{M(site)} + \mathrm{H}^+ + \mathrm{e}^- \underset{k_{-1}}{\overset{k_1}{\rightleftarrows}} \mathrm{MH(ads)} \tag{1}$$

$$\mathrm{MH(ads)} + \mathrm{H}^+ + \mathrm{e}^- \underset{k_{-2}}{\overset{k_2}{\rightleftarrows}} \mathrm{M(site)} + \mathrm{H}_2 \tag{2}$$

$$2\mathrm{MH(ads)} \underset{k_{-3}}{\overset{k_3}{\rightleftarrows}} 2\mathrm{M(site)} + \mathrm{H}_2 \tag{3}$$

$$\mathrm{MH(ads)} \underset{k_{-4}}{\overset{k_4}{\rightleftarrows}} \mathrm{H(abs)} + \mathrm{M(site)} \tag{4}$$

The kinetics, making the usual assumption about Langmuir adsorption, are given by Eqs. (5)-(8), where the rate constants for the electron-transfer steps have the usual Tafel-like potential dependence. The fractional concentration of H in the metal is $X = c/c_{\mathrm{max}}$, and X_0 is its value just inside the metal. Subsequently, the absorbed H diffuses into the metal, and in the case of a Devanathan-Stachurski cell, is oxidized on the exit side.

$$v_1 = k_1(1-\theta) - k_{-1}\theta \tag{5}$$

$$v_2 = k_2\theta - k_{-2}(1-\theta) \tag{6}$$

$$v_3 = k_3\theta^2 - k_{-3}(1-\theta)^2 \tag{7}$$

$$v_4 = k_4\theta(1-X_0) - k_{-4}(1-\theta)X_0 \tag{8}$$

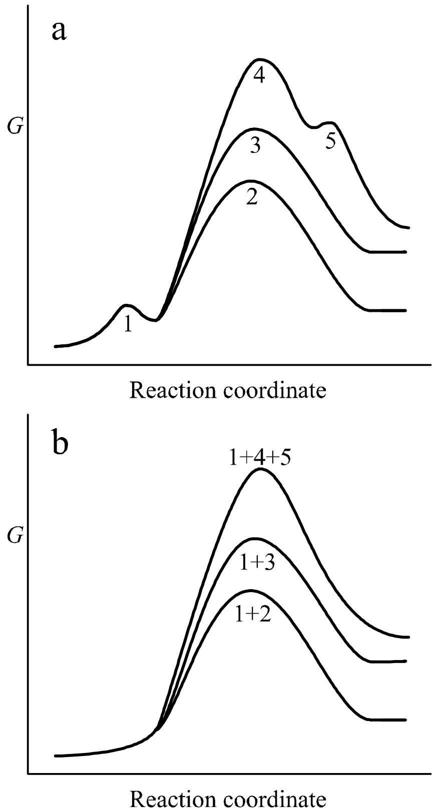

Figure 1: Schematic Gibbs energy profiles for the mechanism of Eqs. (1)-(4). Numbers indicated reaction steps. Step 5 represents unspecified subsequent steps for absorbed hydrogen, such as diffusion through the metal and oxidation at the exit side. (a) unsimplified mechanism, (b) simplified incorporating step 1 as a fast preequilibrium step and step(s) 5 as much faster than step 4.

The govening equations (9) and (10) describe the net rates of production of the adsorbed and absorbed species, where Γ_{m} is the concentration (mol m^{-2}) of adsorption sites on the clean surface and J_X is the flux of X into the metal at the metal surface. Once these equations are solved for the conditions of interest, then the Faradaic current is calculated from Eq. (11).

$$\Gamma_{\mathrm{m}}\mathrm{d}\theta/\mathrm{d}t = r_\theta = v_1 - v_2 - 2v_3 - v_4 \tag{9}$$

$$J_X = r_X = v_4 \tag{10}$$

$$j_{\mathrm{f}}/F = r_{\mathrm{e}} = -v_1 - v_2 \tag{11}$$

1.1. Step 1 preequilibrium

Consider now the simplification where step 1 is considered as a preequilibrium step, to be followed by the relatively slower steps 2, 3, and 4, which are parallel reactions that can be considered competitive and jointly rate determining. That is, there are three pathways, each consisting of step 1 as a preequilibrium step and one of the other steps as a following rate-determining step. A schematic of the Gibbs energy profiles is given in Fig. 1. The fast step 5 after the RDS is dealt with by the steady-state approximation as described earlier [9].

As a first consequence of the assumption of quasithermodynamic equilibrium for step 1, the electrochemical equilibrium constant K_1 can appear in a final rate expression, but not the rate v_1 or the kinetic parameters for step 1: k_1, k_{-1} or the symmetry factor β_1. The symmetry factor cancels in the ratio of rate constants $K_1 = k_1/k_{-1}$, and the potential dependence of θ is determined solely by the potential dependence of the equilibrium constant, Eqs. (12) and (13):

$$K_1 = K_1^{\mathrm{eq}} \exp\left(-\frac{F\,(E-E_r)}{RT}\right) = \frac{\theta}{1-\theta} \tag{12}$$

$$\theta = \frac{K_1}{1+K_1} = \theta(E) \tag{13}$$

Therefore a second consequence of this choice is that θ may be eliminated from the rate expressions in favour of potential. The derivative $\mathrm{d}\theta/\mathrm{d}E$ from Eq. (12) may be converted to a pseudocapacitance, Eq. (14), where the negative sign has been added to make C positive.

$$C = -\Gamma_{\mathrm{m}} F\,\mathrm{d}\theta/\mathrm{d}E \tag{14}$$

Elimination of the rate parameters can be done by eliminating v_1 from Eqs. (9)-(11), simply by adding Eqs. (9) and (11). Then the chain rule $\mathrm{d}\theta/\mathrm{d}t = (\mathrm{d}\theta/\mathrm{d}E)\,(\mathrm{d}E/\mathrm{d}t)$ leads to:

$$j_{\mathrm{f}} = C\,\mathrm{d}E/\mathrm{d}t + F\,(-2v_2 - 2v_3 - v_4) \tag{15}$$

At steady state, $\mathrm{d}E/\mathrm{d}t = 0$, the current density is $j_{\mathrm{f}} = F(-2v_2 - 2v_3 - v_4)$, and so the above just formalizes the fact that two electrons flow every time step 2 progresses, two electrons flow every time step 3 progresses, and one electron flows every time step 4 progresses. This combination of rates is an apparent rate of production of electrons, $\widehat{r}_{\mathrm{e}}$, Eq. (16). Here the caret is used to indicate the use of an approximation (the preequilibrium approximation) where there is possible ambiguity.

$$\widehat{r}_{\mathrm{e}} = -2v_2 - 2v_3 - v_4 \tag{16}$$

If the coverages are replaced by their expressions in terms of potential through Eq. (13), e.g., $v_4 = k_4K_1/(1+K_1)$, then the problem is completely formulated without explicit mention of θ:

$$j_{\mathrm{f}} = C\,\mathrm{d}E/\mathrm{d}t + F\widehat{r}_{\mathrm{e}}(E, X_0) \tag{17}$$

1.1.1. *Low-concentration absorbed hydrogen*

An additional simplification gives the simplest case. If X_0 is assumed to be small, then v_4 simplifies to $k_4\theta$, with the consequence that the concentration of absorbed H and its diffusion do not enter the kinetics: $\widehat{r}_{\mathrm{e}}$ depends only on potential and Eq. (10) is not required. The Faradaic admittance is then found by linearizing Eq. (17) and converting to phasors in the usual way; the time derivative $\mathrm{d}E/\mathrm{d}t$ becomes $\mathrm{i}\omega\widetilde{E}$.

$$\widetilde{j}_{\mathrm{f}} = \mathrm{i}\omega C\,\widetilde{E} + F\frac{\mathrm{d}\widehat{r}_{\mathrm{e}}}{\mathrm{d}E}\widetilde{E} \tag{18}$$

$$Y_{\mathrm{f}} = \widetilde{j}_{\mathrm{f}}/\widetilde{E} = \mathrm{i}\omega C + \widehat{R}_{\mathrm{ct}}^{-1} \tag{19}$$

The Faradaic admittance is a parallel combination of the pseudocapacitance C and the apparent charge-transfer resistance $\widehat{R}_{\mathrm{ct}}$. The two-semicircle impedance characteristic of single-adsorbed mechanisms has reduced to a single semicircle. To understand the apparent absence of adsorbed species intuitively, note that the prequilibrium step can be combined with the subsequent step to give a single effective reaction from the reactants to the transition state for the respective RDS (Fig. 1). For the three pathways here, this means the impedance is that of the adsorptionless reactions:

$$2\mathrm{H}^+ + 2\mathrm{e}^- \xrightarrow{K_1k_2} \mathrm{H}_2 \tag{20}$$

$$2\mathrm{H}^+ + 2\mathrm{e}^- \xrightarrow{K_1^2k_3} \mathrm{H}_2 \tag{21}$$

$$\mathrm{H}^+ + \mathrm{e}^- \xrightarrow{K_1k_4} \mathrm{H(abs)} \tag{22}$$

Here, the effective rate constants above the reaction arrows are the simple ones obtained in the low coverage case $\theta \approx K_1 \ll 1$ and will be more complicated for the high-coverage case. An interesting aspect of this treatment is that although k_4 is usually assumed to be potential independent because of the lack of charge transfer in step 4 (Eq. (4)), the effective rate constant in the approximate treatment is potential dependent through the incorporation of the potential-dependent coverage into the effective rate constant.

The true charge-transfer resistance is defined by IUPAC to be the reciprocal of the partial derivative of the Faradaic current density with respect to potential, fixing all concentrations at the interface [24]; in this case $R_{\mathrm{ct}}^{-1} = F\,(\partial r_{\mathrm{e}}/\partial E)_\theta$. How is the apparent charge-transfer resistance of the simplified mechanism related to the true charge-transfer resistance? Step 1 was eliminated by adding Eqs. (9) and (11), so $\widehat{r}_{\mathrm{e}} = r_{\mathrm{e}} + r_\theta$ and differentiation with respect to E gives Eqs. (23)-(25).

$$\begin{aligned}\widehat{R}_{\mathrm{ct}}^{-1} = F\frac{\mathrm{d}\widehat{r}_{\mathrm{e}}}{\mathrm{d}E} &= F\left(\frac{\partial r_{\mathrm{e}}}{\partial E}\right)_\theta + F\left(\frac{\partial r_{\mathrm{e}}}{\partial \theta}\right)_E\frac{\mathrm{d}\theta}{\mathrm{d}E}\\ &\quad + \left[F\left(\frac{\partial r_\theta}{\partial E}\right)_\theta + F\left(\frac{\partial r_\theta}{\partial \theta}\right)_E\frac{\mathrm{d}\theta}{\mathrm{d}E}\right] \qquad (23)\\ &= F\left(\left(\frac{\partial r_{\mathrm{e}}}{\partial E}\right)_\theta + \left(\frac{\partial r_{\mathrm{e}}}{\partial \theta}\right)_E\frac{\mathrm{d}\theta}{\mathrm{d}E}\right) \qquad (24)\\ &= R_{\mathrm{ct}}^{-1} + F\left(\frac{\partial r_{\mathrm{e}}}{\partial \theta}\right)_E\frac{\mathrm{d}\theta}{\mathrm{d}E} \qquad (25)\end{aligned}$$

(The combination of derivatives in square brackets in Eq. (23) is zero, which may be derived from the fact that the steady-state θ is found by solving $r_\theta = 0$.) The second

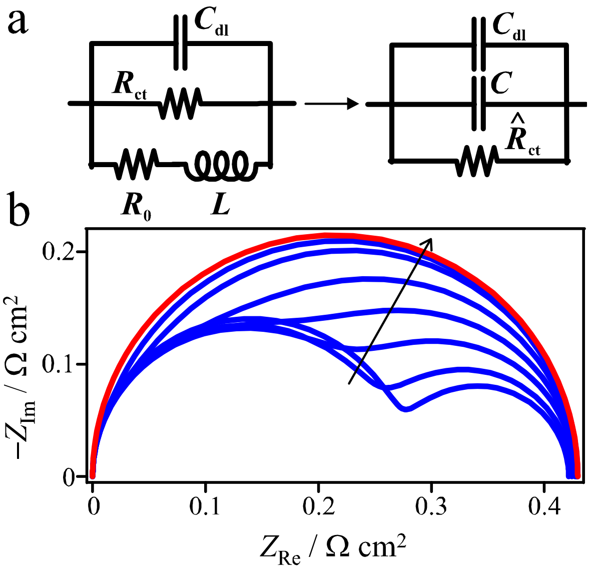

Figure 2: Step 1 and 2 mechanism with step 1 approaching equilibium. (a) Full equivalent circuit (left) becomes approximate equivalent circuit (right). (b) Full impedance spectra (Eq. (26), blue) evolve toward the approximate spectrum (Eq. (19), red). $E - E_r = -0.2$ V, $C_{\mathrm{dl}} = 20$ μF cm^2, rate constants (mol cm^{-2} s^{-1}) at -0.2 V: $k_1/k_{-1} = 1.20 \times 10^{-4}$, $k_2 = 1.03 \times 10^{-6}$, $k_{-2} = 2.15 \times 10^{-9}$, $10^9 k_{-1} =$ 1, 2, 5, 10, 20, 50, 100.

term in Eq. (25) is the adjustment for the fact that the coverage θ is not actually fixed but is oscillating too rapidly to be detected. The two terms of Eq. (25) directly correspond to elements of the the inductive equivalent circuit that applies for a single-adsorbed intermediate mechanism [25] (Fig. 2a). This circuit has the admittance of Eq. (26), where R_0 and L are negative for a capacitive adsorption semicircle.

$$Y_{\mathrm{f}} = R_{\mathrm{ct}}^{-1} + \frac{1}{\mathrm{i}\omega L + R_0} \tag{26}$$

In the simplified circuit, it is evident that $\widehat{R}_{\mathrm{ct}}$ is equal to the zero-frequency resistance (polarization resistance), so that Eq. (25) may be written in terms of R_0, Eq. (27).

$$\widehat{R}_{\mathrm{ct}}^{-1} = R_{\mathrm{ct}}^{-1} + R_0^{-1} \tag{27}$$

For the usual case of negative R_0, the apparent charge-transfer resistance is larger than the true charge-transfer resistance. Consideration of Eqs. (26) and (27) suggests the simplification results in decreasing L. This is verified in the series of plots in Fig. 2b for the impedance of the mechanism with only steps 1 and 2. The ratio k_1/k_{-1} is fixed at 1.2×10^4, and then k_1 and k_{-1} are increased, making step 1 tend toward a true equilibrium. As the rate constants increase by a factor of 100, the value of $-L$ decreases from 1.3×10^{-4} to 9.0×10^{-7} H cm^2, and the two semicircles merge to agree with the approximate treatment (red curve). In this range of rate constants, R_{ct} changes only by 20% (from 0.28 to 0.24 Ω cm^2) and R_0 changes only by 60%, while their parallel combination changes only by 2%. The high equilibrium constant means that the coverage is very close to unity, which makes the pseudocapacitance comparable to or smaller than a double layer value. Therefore, the measured capacitance, which is the sum $C + C_{\mathrm{dl}}$, might be mistaken for a double-layer capacitance. In other words, the simplified mechanism could be easily confused with an adsorptionless mechanism, despite there being full coverage of intermediate on the surface.

1.1.2. High-concentration absorbed hydrogen

Consider now the case of where the kinetics for step 4 depend on the absorbed hydrogen concentration, while still retaining the preequilibrium assumption for step 1. Eqs. (10) and (16) still apply, with $\widehat{r}_{\mathrm{e}}$ and $\widehat{r}_{\mathrm{X}}$ depending now on both E and X_0, and the governing equations are therefore Eqs. (17) and (28).

$$J_X = \widehat{r}_X(E, X_0) \tag{28}$$

where as before the carets indicate the θ-dependence has been converted to potential dependence using Eq. (13). Converting to impedance, $C\,\mathrm{d}E/\mathrm{d}t$ will generate a pseudocapacitance in parallel to the Faradaic admittance of the simpler problem fomulated without θ. The apparent charge-transfer resistance, Eq. (29), will be calculated fixing the concentration X_0, but not the coverage θ whose time variation has already been incorporated into the rate constants. It can be related to the true charge-transfer resistance in the same way as before, though it is no longer equal to the polarization resistance.

$$\widehat{R}_{\mathrm{ct}}^{-1} = F\left(\frac{\partial \widehat{r}_{\mathrm{e}}}{\partial E}\right)_{X_0} = F\left(\frac{\partial r_{\mathrm{e}}}{\partial E}\right)_{\theta, X_0} + F\left(\frac{\partial r_{\mathrm{e}}}{\partial \theta}\right)_{X_0, E}\frac{\mathrm{d}\theta}{\mathrm{d}E} \tag{29}$$

$$= R_{\mathrm{ct}}^{-1} + F\left(\frac{\partial r_{\mathrm{e}}}{\partial \theta}\right)_{X_0, E}\frac{\mathrm{d}\theta}{\mathrm{d}E} \tag{30}$$

As an specific example, H diffusion through a metal foil in a Devanathan-Stachurski cell with rapid oxidation of H at the exit side leads to a finite-length diffusion element (short Warburg) [19]. Explicit calculation of the impedances for the full and approximate cases by the usual methods [1–4] gives the equivalent circuits of Figs. 3a and 3b, where the circuit elements are related to the kinetic parameters as described in appendix A.

As before, the simplification removes the inductor and adds the pseudocapacitance. The semicircle corresponding to adsorption disappears from the impedance spectrum, a case already discussed by Lasia (Fig. 6, Ref. 19) though not explicitly in terms of equivalent circuits.

1.1.3. Step 4 preequilibrium

A common case in the literature is to consider the hydrogen ingress as an equilibrium step. Then steps 1 and 4 are preequilibria and the diffusion is rate limiting. The equilibrium coverage θ is still given by Eq. (13) and the equilibrium concentration X_0 can be calculated as in Eqs. (31)-(33). Both X_0 and θ will now oscillate in phase with

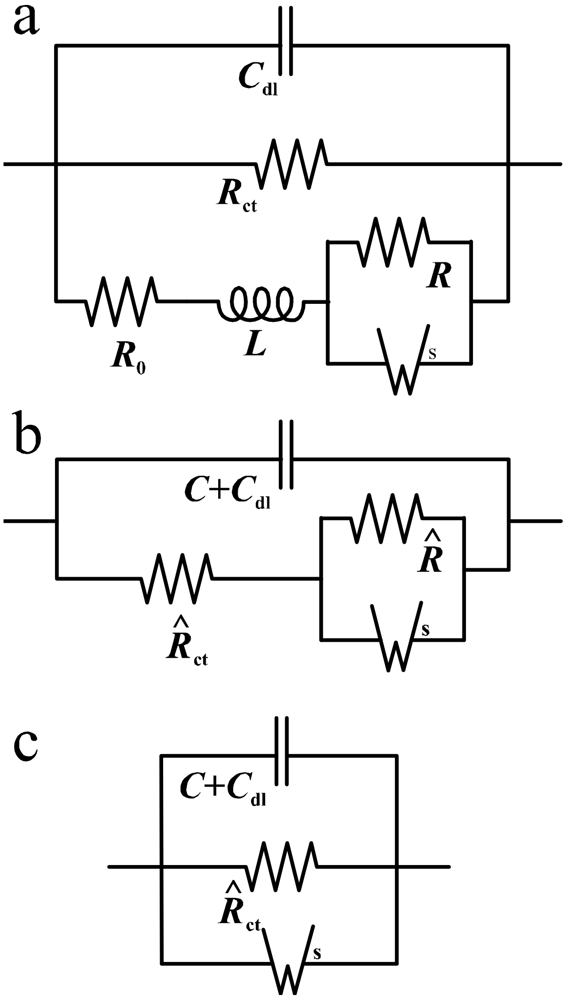

Figure 3: Equivalent circuits with finite diffusion of absorbed H. (a) Full equivalent circuit, (b) Approximate equivalent circuit with step 1 preequilibrium, (c) Approximate equivalent circuit with steps 1 and 4 as equilibria.

the potential. Although K_4 is potential independent, the oscillations in θ cause oscillations in X_0 in order to maintain K_4 constant, explaining the presence of K_1 in Eq. (33).

$$K_4 = \frac{X_0\,(1-\theta)}{\theta(1-X_0)} \tag{31}$$

$$K_4/K_1 = \frac{X_0}{1-X_0} \tag{32}$$

$$X_0 = \frac{K_4/K_1}{1+K_4/K_1} \tag{33}$$

The governing equations need to be rewritten without v_1 and v_4, which can be achieved by using Eq. (10) in Eq. (15)

$$j_{\mathrm{f}} = C\,\mathrm{d}E/\mathrm{d}t + F\,(-2v_2 - 2v_3) - FJ_X \tag{34}$$

$$= C\,\mathrm{d}E/\mathrm{d}t + F\widehat{r}_{\mathrm{e}} - FJ_X \tag{35}$$

This leads to the Faradaic impedance of Eq. (36), which is a parallel combination of the pseudocapacitance, an apparent charge-transfer resistance, and the finite Warburg element (Fig. 3c).

$$\widehat{Y}_{\mathrm{f}} = \widehat{R}_{\mathrm{ct}}^{-1} + \mathrm{i}\,\omega C + \widehat{Z}_{\mathrm{W}}^{-1} \tag{36}$$

It is interesting that the pseudocapacitance is the same as before: only the adsorbed species "stores charge" at the interface. This is because in this conventional formulation of the kinetics the subsurface absorbed hydrogen is not considered as a separate species from the diffusing species. The apparent charge-transfer resistance is still related to the true charge-transfer resistance through Eq. (30), but now $\widehat{r}_{\mathrm{e}} = -2v_2 - 2v_3$ and it seems as though the electron associated with generating the absorbed species is not counted. In fact the subsurface diffusing species cannot truly be in equilibrium with the adsorbed species unless there is no diffusion gradient, so the expression for the equilibrium constant in Eq. (31) can only be an approximation. A resolution to this issue is to elevate the subsurface absorbed species with concentration X_0 to the status of an "adsorbed" species with its own governing equation $\Gamma'_{\mathrm{m}}\mathrm{d}X_0/\mathrm{d}t = v_4 - v_5$, where new step 5 "desorbs" X_0 into the bulk metal, with $J_X = v_5$. Consideration of this case (still with step 4 at equilibrium) leads to $\widehat{r}_{\mathrm{e}} = -2v_2 - 2v_3 - v_5$ and inclusion of X_0 into the pseudocapacitance, but the equivalent circuit of Fig. 3c still applies. In either formulation, the impedance shows little hint of adsorption, with the possible exception that $C + C_{\mathrm{dl}}$ may be large enough to suggest a pseudocapacitance. Therefore, it may be confused with the case of direct absorption, in which hydrogen ingress occurs without passing through an adsorbed state.

2. Conclusions

Some example cases have been used to illustrate a general strategy for inclusion of preequilibrium steps into the govening equations in order to simplify derivation of the impedance and related equivalent circuits. The charge-transfer resistance is an apparent one that differs from the true charge-transfer resistance found from the unsimplified kinetics. The cases presented show examples where adsorption may be operating, but this is not evident in the impedance spectrum. Aside from giving a deeper insight into the nature and meaning of impedance for reaction mechanisms, directly deriving simplified impedances with fewer parameters facilitates fitting of impedance to experimental data.

3. Acknowledgements

I thank the Natural Sciences and Engineering Research Council of Canada (Discovery grant RGPIN-2017-04045) for financial support of this work.

Appendix A

The equivalent circuit in Fig. 3a differs from the published circuit given by Lasia [19] (Fig. 5). The relationships between the circuit elements and the kinetic partial derivatives may be derived from Eqs. (9) - (11) in the usual way [1–4] and are given by Eqs. (37) - (42), where d is the thickness of the foil through which absorbed H diffuses with diffusivity D.

$$R_{\mathrm{ct}}^{-1} = F\left(\frac{\partial r_{\mathrm{e}}}{\partial E}\right)_{\theta,X_0} \tag{37}$$

$$R_0 = -F^{-1}\left(\frac{\partial r_\theta}{\partial \theta}\right)_{E,X_0}\left[\left(\frac{\partial r_\theta}{\partial E}\right)_{\theta,X_0}\left(\frac{\partial r_{\mathrm{e}}}{\partial \theta}\right)_{E,X_0}\right]^{-1} \tag{38}$$

$$L = F^{-1}\Gamma_{\mathrm{m}}\left[\left(\frac{\partial r_\theta}{\partial E}\right)_{\theta,X_0}\left(\frac{\partial r_{\mathrm{e}}}{\partial \theta}\right)_{E,X_0}\right]^{-1} \tag{39}$$

$$\tau^{-1} = R_0/L = -\Gamma_{\mathrm{m}}^{-1}\left(\frac{\partial r_\theta}{\partial \theta}\right)_{E,X_0} \tag{40}$$

$$\begin{aligned} R = {} & F^{-1}\left(\frac{\partial r_X}{\partial \theta}\right)_{E,X_0}\left(\frac{\partial r_\theta}{\partial X}\right)_{E,\theta} \times \\ & \left[\left(\frac{\partial r_X}{\partial X}\right)_{E,\theta}\left(\frac{\partial r_\theta}{\partial E}\right)_{\theta,X_0}\left(\frac{\partial r_{\mathrm{e}}}{\partial \theta}\right)_{E,X_0}\right]^{-1} \end{aligned} \tag{41}$$

$$Z_{\mathrm{W}} = -R\left(\frac{\partial r_X}{\partial X}\right)_{E,\theta} c_{\mathrm{max}}^{-1}\tanh\left(d\sqrt{\mathrm{i}\,\omega/D}\right)/\sqrt{\mathrm{i}\,\omega D} \tag{42}$$

For the simplified circuit of Fig. 3b, the governing equations Eqs. (17) and (28) lead to:

$$\widehat{R}_{\mathrm{ct}}^{-1} = F\left(\frac{\partial \widehat{r}_{\mathrm{e}}}{\partial E}\right)_{X_0} \tag{43}$$

$$\widehat{R}^{-1} = -\widehat{R}_{\mathrm{ct}}^{-1} + \widehat{R}_1^{-1} \tag{44}$$

$$\widehat{Z}_{\mathrm{W}} = -\widehat{R}_1\left(\frac{\partial \widehat{r}_X}{\partial X}\right)_{E} c_{\mathrm{max}}^{-1}\tanh\left(d\sqrt{\mathrm{i}\,\omega/D}\right)/\sqrt{\mathrm{i}\,\omega D} \tag{45}$$

$$\widehat{R}_1 = F\widehat{R}_{\mathrm{ct}}^2\left(\frac{\partial \widehat{r}_{\mathrm{e}}}{\partial X}\right)_{E}\left(\frac{\partial \widehat{r}_X}{\partial E}\right)_{X}\left(\frac{\partial \widehat{r}_X}{\partial X}\right)_{E}^{-1} \tag{46}$$

References

[1] D.A. Harrington, P. van den Driessche, Mechanism and equivalent Circuits in EIS, Electrochim. Acta 56 (2011) 8005.

[2] D.A. Harrington, Electrochemical impedance of multistep mechanisms: mechanisms with diffusing species, J. Electroanal. Chem. 403 (1996) 11-24.

[3] D.A. Harrington, Electrochemical impedance of multistep mechanisms: A general theory, J. Electroanal. Chem. 449 (1998) 9-28.

[4] D.A. Harrington, Electrochemical impedance of multistep mechanisms: Mechanisms with static species, J. Electroanal. Chem. 449 (1998) 29-37.

[5] D.A. Harrington, P. van den Driessche, Stability and electrochemical impedance of mechanisms with a single adsorbed species, J. Electroanal. Chem. 501 (2001) 222-234.

[6] J. Sengoku, M. Naito, H. Okamoto, T. Ogita, S. Ichikawa, On the visibility of fast reactions in electrochemical impedance spectroscopy, Chem. Phys. Lett. 525-526 (2012) 125-128.

[7] J. O'M Bockris, Z. Nagy, J. Chem. Ed. 50 (1973) 839.

[8] J. O'M. Bockris, A.K.N. Reddy, Modern Electrochemistry, Plenum Press, New York, 1970, vol. 2, ch. 9.

[9] D.A. Harrington, The rate-determining step in electrochemical impedance spectroscopy, J. Electroanal. Chem., 737 (2015) 30-36.

[10] J.P. Diard, B. Le Gorrec, C. Montella, Impedance zone diagram of an oxidation mechanism in and adsorbed phase with chemical recombination, J. Electroanal. Chem. 161 (1984) 235-245.

[11] J.-P. Diard, P. Landaud, B. Le Gorrec, C. Montella, Calculation, simulation and interpretation of electrochemical impedance. Part II. Interpretation of Volmer-Heyrovsky impedance diagrams, J. Electroanal. Chem. 255 (1988) l-20.

[12] J.-P. Diard, Le Gorrec, C. Montella, Calculation, simulation and interpretation of electrochemical impedances 3. Conditions for observation of low-frequency inductive diagrams for a 2-step electron-transfer with an adsorbed intermediate species, J. Electroanal. Chem. 326 (1993) 13-36.

[13] J.-P. Diard, B. Le Gorrec, C. Montella, C. Montero-Ocampo, Calculation, simulation and interpretation of electrochemical impedance. Part IV. Second order electrochemical impedances, J. Electroanal. Chem. 352 (1993) 1-15.

[14] J.-P. Diard, B. Le Gorrec, C. Montella, Discussion of first-order inductive impedance for the Volmer-Heyrovsky mechanism, J. Chim. Phys. 92 (1995) 656–667.

[15] M.B. Molina Concha, M. Chatenet, C.Montella, J.-P. Diard, A Faradaic impedance study of E-EAR reaction, J. Electroanal. Chem. 696 (2013)24–37.

[16] V.I. Kichigin, A.B. Shein, Diagnostic criteria for hydrogen evolution mechanisms in electrochemical impedance spectroscopy, Electrochim. Acta, 138 (2014) 325-333.

[17] A. Lasia, Mechanism and kinetics of the hydrogen evolution reaction, Int. J. Hydrogen Energy 36 (2019) 19484-19518.

[18] D.A. Harrington, P. van den Driessche, Impedance of Multistep Mechanisms: Equivalent Circuits at Equilibrium, Electrochim. Acta 44 (1999) 4321-4329.

[19] A. Lasia, Applications of electrochemical impedance spectroscopy to hydrogen adsorption, evolution and absorption into metals, in: B.E. Conway, R.E. White (Eds.), Modern Aspects of Electrochemistry, v. 35, Kluwer Academic/Plenum, New York, 2002, pp. 1-49.

[20] J.S. Chen, J.-P. Diard, R. Durand, C. Montella, Hydrogen insertion reaction with restricted diffusion. Part 1. Potential step-EIS theory and review for the direct insertion mechanism, J. Electroanal. Chem. 406 (1996) 1-13.

[21] C. Gabrielli, G. Maurin, L. Mirkova, H. Perrot, B. Tribollet, Transfer function analysis of hydrogen permeation through a metallic membrane in a Devanathan cell. I. Theory, J. Electroanal. Chem. 590 (2006) 1-14.

[22] S.Y. Qian, B.E. Conway, G. Jerkiewicz, Kinetic rationalization of catalyst poison effects on cathodic H sorption into metals : relation of enhancement and inhibition to H coverage, J. Chem. Soc. Faraday Trans., 94 (1998) 2945-2954.

[23] V.I. Kichigin, A.B. Shein, Influence of hydrogen absorption on the potential dependence of the Faradaic impedance parameters of hydrogen evolution reaction, Electrochim. Acta, 201 (2016) 233-239.

[24] M. Sluyters-Rehbach, Pure Appl. Chem. 66 (1994) 1831.

[25] D.A. Harrington, B.E. Conway, Electrochim. Acta 32 (1987) 1703.